Proceedings of the IASS 2024 Symposium
Redefining the Art of Structural Design
August 26-30, 2024, Zurich Switzerland
Philippe Block, Giulia Boller, Catherine DeWolf,
Jacqueline Pauli, Walter Kaufmann (eds.)

A study of internal stiffeners in wooden slab panels obtained by topology optimisation

Jiayi Kayee Li*, Markus Matthias Hudert[a], Lars Vabbersgaard Andersen[a]

[a,*] Department of Civil and Architectural Engineering, Aarhus University
8000 Aarhus, Denmark
kayeeli@cae.au.dk

Abstract

Engineered wood products (EWPs) have significantly increased the use of timber structures in buildings for various purposes. To contribute to the development of a circular economy in the building industry, design solutions that can improve material consumption efficiency and construction with waste materials from the production line should be proposed. This work presents a novel internal stiffener design for timber floor slabs. The Finite Element Analysis (FEA) panel model created in Abaqus considers the floor slab boundary conditions applied to volumetric timber modules. Subsequently, the topology optimisation algorithm will be used to generate an optimised solution for the initial solid slab model. This will be followed by a discussion on how the different material resources of discarded wood can be used to produce optimised designs. The primary objective of this study is to provide a solution to mitigate production waste in wood construction. The optimisation results provided will serve as a reference for future research on the construction of wooden stiffeners using leftover wood items. The ultimate goal is to achieve a circular economy in timber buildings by utilising discarded wood resources.

Keywords: Timber design, circular design, topology optimisation, construction waste, wooden floor slabs.

1. Introduction

According to the findings of a study that benchmarked the life cycle of buildings, the fabrication of floor slabs is responsible for the greatest proportion of greenhouse gas emissions throughout the life of the building [1]. This conclusion has been drawn attributed to the insufficient utilisation of floor slab materials. In conventionally designed projects, floor slabs usually account for about half of all materials used. As indicated by studies on the carbon content of construction concrete components, the current utilisation of concrete structural elements is frequently found to be below 60 percent [2]. The usage of wood as a substitute for concrete in the material selection has the potential to substantially mitigate the adverse effects of greenhouse gas emissions, since timber has a low global warming potential [3]. Nevertheless, its supply is limited, and the design of wooden floor slabs needs to be optimised to conserve manufacturing materials and reduce environmental impacts. In addition, prospective research could investigate measuring the impact of upcycling waste wood into floor slabs and investigate how this impact could be measured already at an early design stage [4].

Currently, the use of precast concrete hollow-core floor slabs enhances the material utilisation. Jipa et al. [5] used three-dimensional (3D) printing to accurately fabricate the topological optimisation outcomes of concrete floor slabs. The prototype employs a reduced amount of material compared to solid concrete slabs while preserving the necessary strength. In relation to the case study about the timber hollow core floor slabs, Schramm et al. [6] proposed various internal support configurations to accommodate diverse circumstances. The designs not only decrease the amount of material required but also minimise the reliance on large beams for structural support. Svatoš-Ražnjević et al. [7] investigated the versatile utilisation of hollow wood panels. The research also explored the viability of exploiting the voids inside the slabs to facilitate the accommodation of integrated building services.

Currently, one of the difficult factors in optimising hollow timber slabs is the placement of the stiffeners. EWPs are designed to utilise the main grain direction for capacity to mitigate the anisotropy of natural wood as a load-bearing material. Therefore, placement and orientation approaches should consider maximising the performance by utilising, the load-carrying capacity of the wood in the main strength direction, i.e., along the grain. Moreover, an investigation is needed to provide an effective positioning of stiffeners within the internal cavity of the product, while ensuring that they possess the necessary load-bearing capacity for infrequent load scenarios. In addition, the present examples utilised for the research are customised designs. It is necessary to propose designs that are expected to be manufactured on a large scale and are suitable for digital fabrication to improve manufacturing efficiency.

The paper illustrates the workflow involved in the production process of timber panels, intending to guide an optimisation strategy. The floor slabs in a volumetric timber module are subject to specific work settings, and the shape of the internal material is determined by a topology optimisation algorithm. The comparison between the optimal results and a solid model with equivalent material volume consumption reveals that the optimised slabs exhibit enhanced capacity, as evidenced by the maximum values of the maximum principal stresses and maximum deflections. The following discussion part presents the feasibility of optimised internal stiffeners using wood manufacturing.

2. Background

To enhance the preparation for optimisation work, this section will provide an analysis of how the existing production process can be integrated with optimisation work to reduce waste. In addition, methods of fabrication for optimised designs will be discussed.

2.1. Avoiding waste in the production process of wood floor slabs

During the production of wall panels, significant amounts of materials are left, for example, as cut-outs for windows and doors. These materials are newly created and can be utilised to bear structural loads. Based on the concept of utilising the internal stiffeners of panel products, the use of leftover parts as internal stiffeners improves material efficiency and saves unnecessary waste. Figure 1 shows the entire process of producing panel products from leftover wood. In this scenario, the internal stiffeners can be designed based on the geometry and qualities of the most common leftover wood items. Some of the icons were redesigned with reference to SVG Repo samples [8].

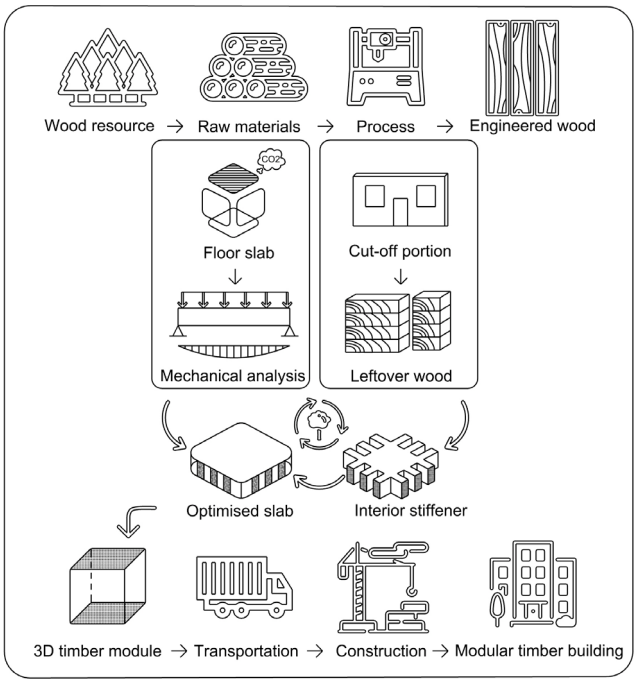

Figure 1: A process for producing internally stiffened panel products using leftover wood.

2.2. Fabrication of topology optimisation algorithms to wooden floor slabs

Currently, topology optimisation results are generated customised to the constraint settings of each scenario. The optimised results exhibit irregularly variable curves along the edges. In such cases, the fabrication of intricate configurations can be a challenge. Vantyghem et al. [9] employed concrete fluidity to accurately construct topologically optimised post-tensioned concrete beams with additive manufacturing techniques. In terms of EWPs, laser cutting and CNC routing are the two utilised digitization techniques for load-bearing wood panels. However, these techniques are subtractive instead of being additive, potentially producing rather than reducing production waste. In any case, when defining the geometry of internal stiffeners, the intrinsic anisotropy of wood and the constructability of the slap must be considered. Hence, additional shape optimisation work must be carried out for wood slabs, using the results of topology optimisation as the starting point.

The schematic of Figure 2 shows the possibilities of fabricating optimised internal wood stiffeners. The internal configurations described are taken from the results of the optimisation work in this paper and are used here as a reference. The first option allows for the use of planking elements, as shown in Figure 2. The internal stiffener can be divided into multiple layers to achieve different patterns. Connections between components can utilise existing solutions suitable for wooden components, such as adhesives, bolts, dowels, and interlocks [10, 11] or hybrid methods. The second method of fabrication is to place stiffeners vertically or at an angle in the interior of the board. This approach saves material and reduces the number of joints. However, it also requires secondary shape optimisation to determine the spatial layout based on the orientation of the material grain.

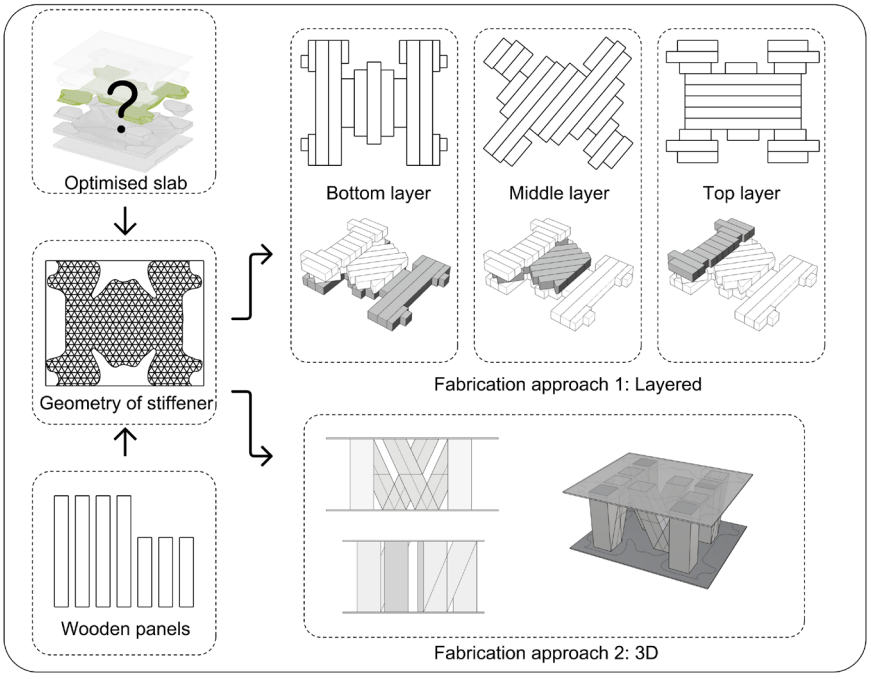

Figure 2: Fabrication approaches of internal stiffeners.

3. Methodology

The application of topology optimisation has been extensively employed in addressing engineering challenges. This section briefly outlines the theory of the algorithm, followed by the introduction of the analysis approach used in this study.

3.1. Topology optimisation algorithm

The results of topology optimisation are related to the design objectives and specified constraints within the design domain area. The optimisation work was carried out using the SIMP (Solid Isotropic Modelling with Penalisation) algorithm, and the mathematical expression in equation [12] below explains the process:

$$\text{min: } C(\boldsymbol{\rho}) = \frac{1}{2}\mathbf{U}^T\mathbf{K}(\boldsymbol{\rho})\mathbf{U} \tag{1}$$

$$\text{s.t.: } \mathbf{K}(\boldsymbol{\rho})\mathbf{U} = \mathbf{F}$$

$$V(\boldsymbol{\rho}) \leq V^*$$

In Eq. (1), the variable C denotes the objective function, which is in the SIMP algorithm put as the strain energy, while $\boldsymbol{\rho}, \mathbf{U}$ represent the design variable vector and displacement vector, respectively. $\mathbf{K}(\boldsymbol{\rho}), V(\boldsymbol{\rho})$ indicate the global stiffness matrix and the volume of the finite-element model, respectively. The first constraint is an equality constraint defining static equilibrium, while the second constraint is an inequality constraint defining the maximum volume, V^*, that can be allowed.

Once the initial geometry has been meshed, the optimisation task starts based on Eq. (1), and the density approach is employed to indicate the calculation outcomes of each finite element. Following each iteration, integration points (or entire elements) denoted as 0 are designated for removal from the model, while the ones denoted as 1 are marked for retention to satisfy the objective requirements. The process of optimisation is repeated iteratively until the outcomes reach convergence.

3.2. Finite element model for topology optimisation analysis

Before starting the topology optimisation work, the finite element model to simulate wood floor panels should be built. In this study, load settings and support criteria will be established to represent the usage conditions of the floor slabs in the volumetric timber module. The exterior dimensions are as follows: span length × slab width × thickness = 3 000 mm × 2 400 mm × 600 mm. The span lengths of the boards were referenced to case studies [13] of volumetric modular timber projects to select a typical size with fewer transport constraints. Panel widths are selected from standard production sizes for engineered panel products. A small slab height of, for example. 200 mm leaves little room for optimising the position and amount of material. Therefore, to have enough space for internal optimisation work, the height was initially set at 600 mm, which will be further explored in future work. Figure 3 displays the geometric illustration of the study model within the coordinate system.

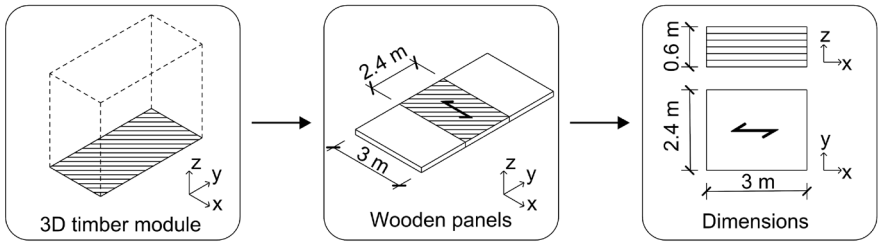

Figure 3: The studied floor slab in 3D timber module.

The model was built in Abaqus as a solid model, and millimetres were used as the modelling unit. An isotropic material with a modulus of elasticity of 12 GPa and a Poisson's ratio of 0.25 was chosen. Since no specific wood type was chosen, the modulus of elasticity selection was used as the common data for wood modelling. This study uses an isotropic material setting for analysis, and it will serve as a form finding reference for subsequent research studying the anisotropic characteristics of wood. A uniformly distributed load of 1 kN/m^2 was applied on the upper surface ($z = 600$ mm). Two rectangular regions with dimensions of 100 mm × 2 400 mm have been defined on the bottom support surface ($z = 0$). These areas are used to simulate the support contact between the wooden walls and the floor slabs in the volumetric module, as depicted in Figure 4. Every node on the support surface is set up to interact with a reference point. Coupling conditions are used and all degrees of freedom of all nodes in the coupling zone are rigidly linked to a single reference point. Boundary conditions are then applied to the reference points on both surfaces. The boundary conditions for the two reference points are defined as $U_y = U_z = UR_x = 0$, i.e., the displacements in the y and z directions as well as the rotation about the x axis are zero. An additional constraint is set to make $U_x = 0$ at reference point 1 to prevent rigid-body motion.

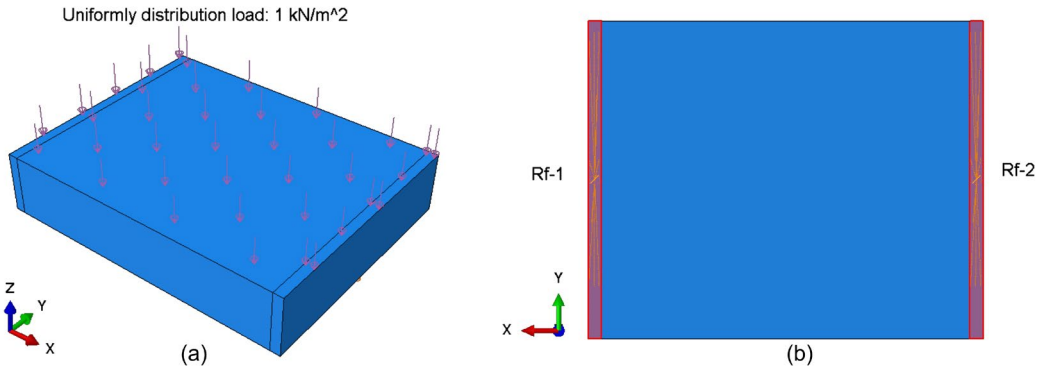

Figure 4: Models in Abaqus. (a) Load conditions. (b) Coupling on constraint surfaces.

During the process of static calculations, the results are achieved by determining the size of the mesh grid using convergence analysis. Three different mesh sizes were chosen for the meshing: 50 mm, 30 mm, and 2 mm. The solid model was meshed into a total of 34 560, 158 400, and 540 000 elements in each of the three scenarios. The maximum principal stress diagram at the section $y = 0$ for the various mesh schemes is displayed in Figure 5. Not surprisingly, the graphic shows that the largest value of the maximum principal stress occurs at the bottom surface $z = 0$.

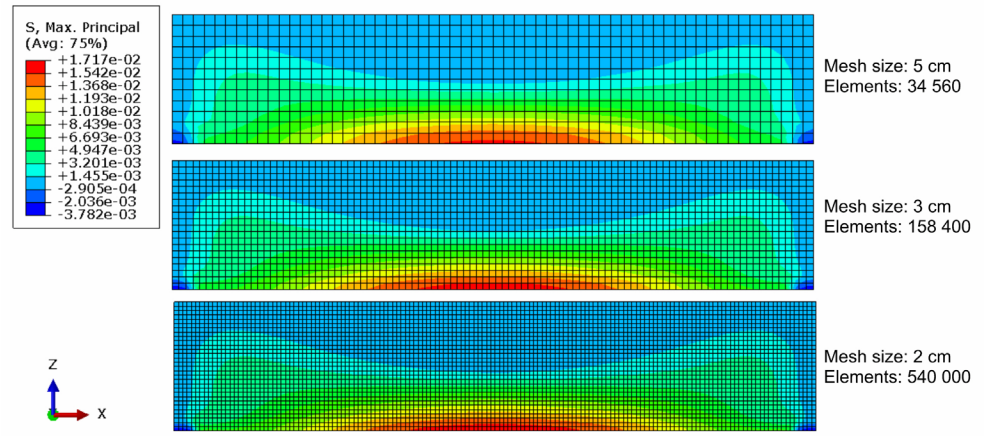

Figure 5: Maximum principal stress (MPa) results at cross-section ($y = 0$).

Figure 6 displays the maximum principal stress values at the chosen nodes on the bottom surface to assess the convergence of the increasingly smaller mesh sizes. The largest relative error between 5 cm and 2 cm results is 5.46%, and 1.94% between 3 cm and 2 cm. A good convergence can be observed based on the relative errors and curves. Considering the computational efficiency, a grid size of 3 cm will be chosen for the following analyses.

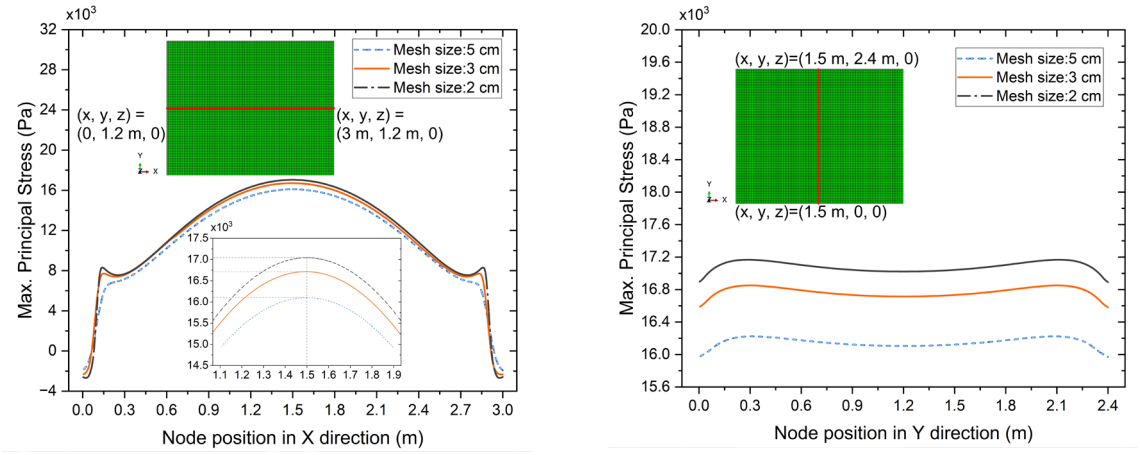

Figure 6: Maximum principal stresses at the nodes chosen on the bottom surface ($z = 0$).

4. Case study

In this section, the tasks and solutions for topology optimisation carried out on the finite element model are described. The outcomes of the topology optimised slab are compared to those of a solid model with an equivalent quantity of material. Following that, the manufacturing of internal stiffeners are discussed in the light of the approaches outlined within the background section. This case study will provide a reference for future optimisation studies considering the anisotropic properties of wood panels.

4.1 Topology optimisation results

For the pre-processing setup of the optimisation work, the target region was set to the entire object and the load region, i.e., the top surface, was frozen. The objective function is set to minimise strain energy across the entire design region. The constrained response is set at 50% of the initial volume. The penalty parameter is 3, and the total number of iterations is set to twenty. Figure 7 illustrates the topology optimisation results for the isometric, top, and right perspectives, respectively. Figure 8 displays the plots of the maximum principal stresses for the optimised model, as seen from the isometric, top, and bottom views.

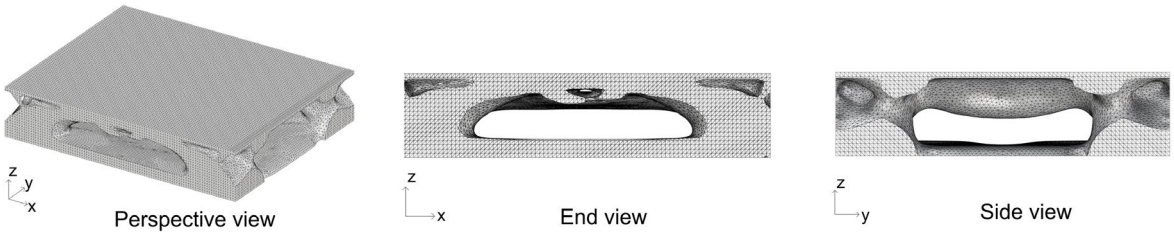

Figure 7: Three views of topology optimisation result obtained with a mesh size of 3 cm.

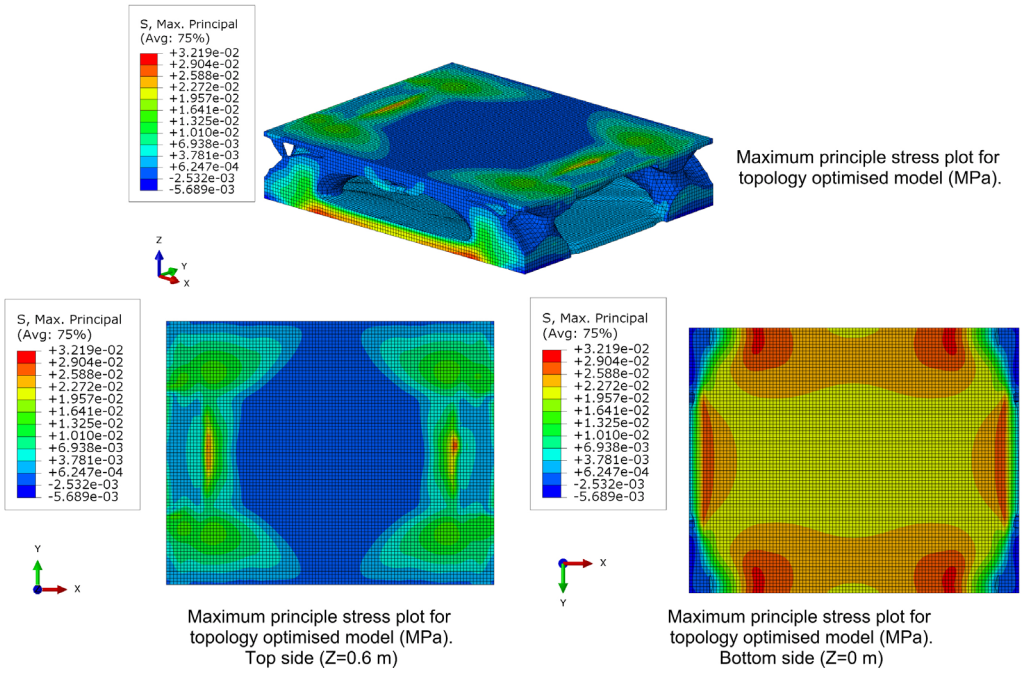

Figure 8: Maximum principal stresses (MPa) results of topology optimisation result.

To demonstrate that the optimisation has not weakened the load-bearing capacity of the slab, a reference solid model was built with the same length and width as the initial model, but with a uniform thickness of 300 mm instead of the 600 mm used as the onset for the optimisation. Thus, the exterior dimensions

of the reference model are 3 000 mm × 2 400 mm × 300 mm. This provides a volume of 2.16 m^3, matching that of the optimised model after cutting away 50% of the material. Figure 9 illustrates an end view of the solid and the optimised model with equal volumes for the comparison of the maximal principal stresses in the two panels.

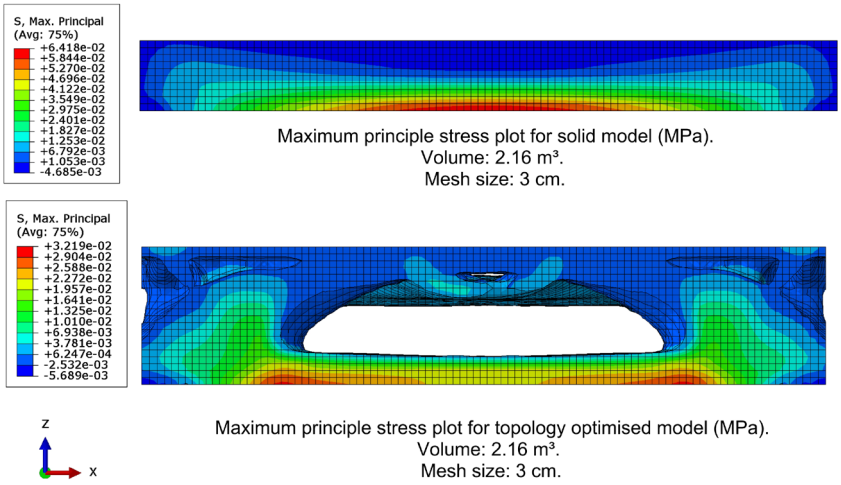

Figure 9: Comparison of the maximum principal stresses (MPa) results in front view (X − Z) for two models.

To further emphasise the greater capacity of the optimised solutions to bear structural loads compared to a solid model of equal volume, Table 1 displays the largest displacement at the bottom of the model ($z = 0$) and the greatest value of the maximum principal stress for the entire slab in each model. The studied displacement and stress of the optimised model are only 19.02% and 50.16%, respectively, of those obtained in the case of the reference solid model.

Table 1. Comparison of solid model and topology optimisation results for the same material volume.

	Scope	Solid model	Topology optimised model
Volume (m^3)	Whole model	2.16	2.16
Max. disp. $U_{z,\,max}$ (mm)	Bottom surface ($z = 0$)	$3.692 \cdot 10^{-2}$	$7.024 \cdot 10^{-3}$
Max. prin. stress σ_{max} (MPa)	Whole model	$6.418 \cdot 10^{-2}$	$3.219 \cdot 10^{-2}$

4.2 Manufacturing analysis of topology optimised wooden slabs

Referring to the proposed fabrication methods mentioned in Section 2.2, the results of this optimisation will be further analysed based on the first method of the layered approach. The mesh unit was 30 mm and the study model was divided into 20 layers along the z-axis. To better understand the internal geometry, every four layers were connected and highlighted as shown in Figure 10.

Since the top surface and support regions of the floor slab were frozen, material could not be removed here. Additionally, the current optimisation results indicate that little material was removed on the bottom surface. Logically, the material is needed here to accommodate normal stresses for optimal performance regarding bending of the slab. The inner part of the volume is filled with material at the four corners of the slab, extending along the z-axis. In contrast, the mid-span section's internal design varies along the z-axis. The remaining material represents the portion of the material that needs to be retained in this scenario. The illustration shows that the design of the panel displays variations in both its thickness and plane. The desired shape can be created by using different sizes of sheet material. Multiple types of panels are combined to account for the various sorts of leftover wood generated by different production lines.

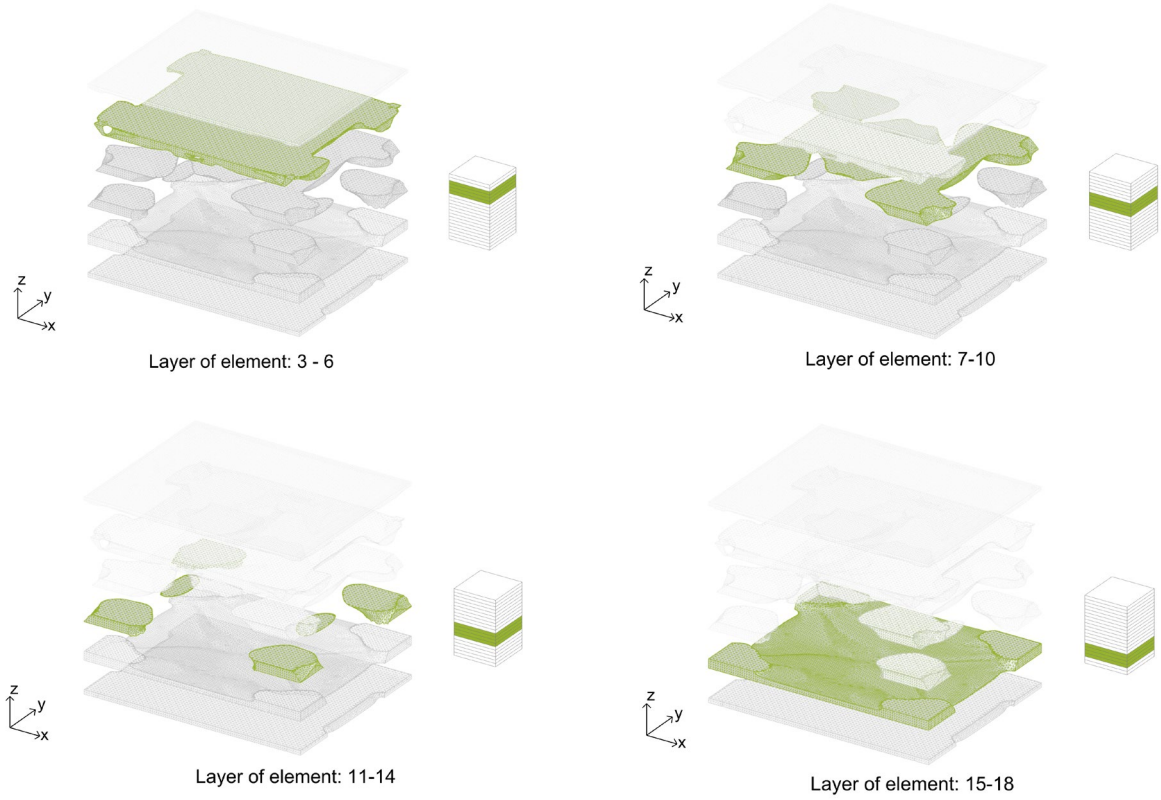

Figure 10: Results of topology optimisation of the interior space as a reference for wooden stiffeners.

5. Discussion and conclusions

The data obtained from the aforementioned comparison between the solid and optimised models is based on models with the same amount of material. It can be concluded that the solid panel conducted an algorithmic process to reset the material distribution based on its stress state after the application of external force. The optimised design showed better load-bearing capability, reflected in smaller values for both maximum deflection and maximum principal stress. However, more performance analyses and comparisons need to be carried out to evaluate this conclusion.

The current optimised internal structure varies across the height of the panel. The profile of the retained material is irregularly curved. However, the algorithm concentrates the remaining materials into regions with higher stress density, and the findings indicate that these zones can be built with solid materials. Residual material can be used as stiffeners to maintain the load-bearing capacity of the panels. These stiffeners can be constructed from various resource materials, such as laminated wood or saw-cut components. In this case study scenario, it is feasible to construct the internal part with board resources. Thicker board materials can be used to create the four corners. This strategy aids in minimising the challenges involved with integrating layered materials.

However, the optimisation outcomes presented in this study were produced based on the specified boundary conditions. It is important to analyse the optimised results for the ultimate limit state and serviceability limit state for more load cases. Optimisation results for both considerations need to be further investigated in order to determine the most useful residual region for internal stiffeners.

In addition to investigating the geometry of the internal stiffeners, further discussion on how to use wood materials for internal design is critical. Given the orthogonal characteristics of the EWPs, the primary grain direction plays an important role in determining the positioning and orientation of the internal stiffeners. Further investigations are intended to be conducted to determine how leftover wood material from different phases of the manufacturing process can be utilised to reshape the optimised interior

stiffeners. Moreover, future studies will look into measuring the impact of upcycling waste wood into floor slabs and investigating how this impact could be measured already at an early design stage.

Acknowledgements

The first author are grateful for the financial support provided by the program of the China Scholarship Council (Grant No. 202209110036).

References

[1] B. Anna, E. Levan, and Q. Kathrin. "Benchmarks for greenhouse gas emissions from building construction."https://static.dgnb.de/fileadmin/dgnb-ev/de/themen/Klimaschutz/Toolbox/2021_DGNB_Study_Benchmarks_for_greenhouse_gas_emissions_from_building_construction.pdf?m=1641813821& (accessed 24 June, 2024).

[2] L. C. C. Group, "Low Carbon Concrete Routemap," Institution of Civil Engineers (ICE), 2022. [Online]. Available: https://www.ice.org.uk/media/q12jkljj/low-carbon-concrete-routemap.pdf

[3] L. Guardigli, "Comparing the environmental impact of reinforced concrete and wooden structures," *Eco-efficient construction and building materials*, pp. 407-433, 2014.

[4] M. Budig, O. Heckmann, M. Hudert, A. Q. B. Ng, Z. Xuereb Conti, and C. J. H. Lork, "Computational screening-LCA tools for early design stages," *International Journal of Architectural Computing*, vol. 19, no. 1, pp. 6-22, 2021.

[5] A. Jipa, M. Bernhard, M. Aghaei Meibodi, and B. Dillenburger, 3D-Printed Stay-in-Place Formwork for Topologically Optimized Concrete Slabs. *Proceedings of the 2016 TxA Emerging Design+ Technology Conference*, pp. 97-107, 2016.

[6] K. Schramm et al., "Redefining Material Efficiency: Computational Design, Optimization and Robotic Fabrication Methods for Planar Timber Slabs," *Design Modelling Symposium Berlin*, pp. 516-527, 2022.

[7] H. Svatoš-Ražnjević, A. Krtschil, L. Orozco, G. Neubauer, J. Knippers, and A. Menges, "Towards design flexibility and freedom in multi-storey timber construction: Architectural applications of a novel, adaptive hollow slab building system," *Proceedings of the World Conference on Timber Engineering (WCTE 2023)*, Norway, pp. 19-22, 2023.

[8] "SVG Repo LLC®." https://www.svgrepo.com/ (accessed April 1, 2024).

[9] G. Vantyghem, W. De Corte, E. Shakour, and O. Amir, "3D printing of a post-tensioned concrete girder designed by topology optimization," *Automation in Construction*, vol. 112, p. 103084, 2020.

[10] C. A. Aranha, M. Hudert, and G. Fink, "Interlocking birch plywood structures," *International Journal of Space Structures*, vol. 36, no. 3, pp. 155-163, 2021.

[11] L. Mangliár and M. Hudert, "Enabling circularity in building construction: Experiments with robotically assembled interlocking structures," *Structures and Architecture A Viable Urban Perspective*: CRC Press, pp. 585-592, 2022.

[12] M. P. Bendsoe and O. Sigmund, Topology optimization: theory, methods, and applications. Springer Science & Business Media, 2013.

[13] J. Li, L. V. Andersen, and M. M. Hudert, "The Potential Contribution of Modular Volumetric Timber Buildings to Circular Construction: A State-of-the-Art Review Based on Literature and 60 Case Studies," *Sustainability*, vol. 15, no. 23, p. 16203, 2023.